Soft Matter

RSC Publishing

PAPER

View Article Online
View Journal | View Issue

Cite this: *Soft Matter*, 2013, **9**, 6254

Janus-like spheres, disks, rings, cylinders, and vesicles from the self-assembly of mixture of AB and BC diblock copolymers in A- and C-selective solvents†

Yuping Sheng,[ab] Xiaoping Yang,[a] Nan Yan[ab] and Yutian Zhu*[a]

Received 4th January 2013
Accepted 29th April 2013

DOI: 10.1039/c3sm00029j

www.rsc.org/softmatter

Janus particles with two different compartments have enormous potential as building blocks of hierarchically multifunctional nanomaterials. One of the most versatile and powerful methods to fabricate Janus micelles is through the solution-state self-assembly of block copolymers. In this study, we applied the Monte Carlo simulation to study the self-assembly of a AB/BC diblock copolymer mixture in A- and C-selective solvents. Our simulations predicted a variety of novel Janus micelles, which include Janus-like cylinders, lamellas, vesicles, and rings, all of which were self-assembled from amphiphilic A_4B_6/B_6C_4 copolymers. The effects of control parameters, which include the solvent quality for solvophobic B blocks (ε_{BS}) and the incompatibility between the solvophilic A and C blocks (ε_{AC}), on the formation of Janus micelles were examined, and a generic phase diagram in $\varepsilon_{BS} \times \varepsilon_{AC}$ was constructed. The phase diagram demonstrates that the micellar shape mainly depends on ε_{BS}, whereas the formation of the Janus architecture is controlled by ε_{AC}. Moreover, the formation pathways of the Janus lamella, vesicle, and ring were investigated and their formation mechanisms were investigated.

Introduction

Janus particles have recently received much attention because of their unique structures and potential applications in nanotechnology such as drug delivery,[1–3] catalysts,[4] microcapsules,[5] nanoprobes,[6,7] and so on. The term "Janus grains" was coined by P. G. de Gennes in his Nobel lecture to represent particles that have two different compartments.[8] Janus particles are generally divided into Janus spheres, disks, cylinders, rings, and vesicles. Fig. 1 shows a schematic of numerous possible Janus architectures. Most Janus particles that have been synthesized are spheres with two discernible hemispheres,[9–13] as shown in Fig. 1a. Recently, several other Janus particles such as Janus cylinders,[14,15] disks,[16,17] and vesicles[18] have also been developed with the architectures illustrated in Fig. 1d, b, and i, respectively. However, other possible Janus architectures shown in Fig. 1 have yet to be synthesized.

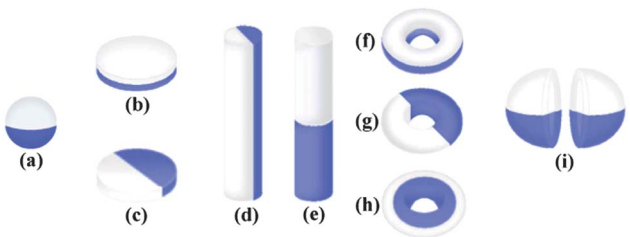

Fig. 1 Various possible Janus micelles: (a) Janus sphere, (b) and (c) Janus disks, (d) and (e) Janus cylinders, (f), (g) and (h) Janus rings, and (i) Janus vesicle.

For the formation of a Janus sphere, it can be easily synthesized *via* the surface modification of pre-existing nanoparticles.[19–21] Recently, several strategies were developed to explore the other possible Janus structures predicted in Fig. 1. One strategy is to firstly generate lamellae-sphere, lamellae-cylinder, or lamellae-lamellar morphologies from the bulk self-assembly of block terpolymers. Selective cross-linking of the central block is then performed, and redissolution leads to the formation of Janus structures wherein the corona is microphase-separated into two distinct domains. Based on this method, Müller and co-workers fabricated Janus spheres,[11] cylinders,[15] and discs[17] using polystyrene-*b*-polybutadiene-*b*-poly(methyl methacrylate) (PS-PB-PMMA) triblock copolymers.

Another strategy to generate Janus particles is through the micellization of block copolymers in solution. In such an approach, ABC triblock copolymers can form Janus micelles in a solution that is selective for A and C blocks.[22] An alternative approach is through the self-assembly of a mixture of AB/BC or AB/CD diblock copolymers in solution. For example, Voets *et al.*

[a]*State Key Laboratory of Polymer Physics and Chemistry, Changchun Institute of Applied Chemistry, Chinese Academy of Sciences, Changchun 130022, People's Republic of China. E-mail: ytzhu@ciac.jl.cn; Fax: +86-43185262126; Tel: +86-43185262866*

[b]*College of Materials Science and Engineering, Jilin University, Changchun 130022, People's Republic of China*

† Electronic supplementary information (ESI) available: Reproducing of Janus cylinder, Janus lamella, Janus vesicle from a different homogeneous initial state. See DOI: 10.1039/c3sm00029j

synthesized a disk-shaped Janus micelle that has a complex coacervate core and a microphase-separated corona from a mixture of poly(acrylic acid)-*b*-poly(acryl amide) (PAA_{42}-*b*-$PAAm_{417}$) and poly(2-methylvinylpyridinium iodide)-*b*-poly(ethylene oxide) ($P2MVP_{42}$-*b*-PEO_{446}) in an aqueous solution.[16] In that study, the electrostatic interaction between PAA and P2MVP ensured the aggregation of two different block copolymers in the same micelle, whereas the subtle repulsion between water-soluble blocks ensured segregation of the corona into two distinct phases. Hu and Liu examined the self-assembly of mixtures of B–C and C–D block copolymers in a solution that was selective for the B and D blocks.[12] They observed a spherical micelle with a two-faced corona. Moreover, Jiang and Han studied the self-assembly of an AB/BC diblock copolymer mixture based on the hydrogen bonding between the two ends of two B blocks.[13] Their simulation results revealed that the resulting micellar architectures, which include Janus micelles, mixed micelles, and pure micelles, depend on the intensity of the associative interaction, the directional dependency of H-bonding, and the intrinsic repulsive interaction between A and C blocks. Very recently, Jiang and coworkers used the same AB/BC blending system to predict a Janus-type asymmetric vesicle based on the micellization of a mixture of block copolymers in a selective solvent.[18]

From previous studies, mixing two different diblock copolymers in a selective solution is an important approach to generate Janus micelles. In these studies,[12,13,16,18] additional interactions (*e.g.*, electrostatic interactions or hydrogen bonding) between blocks in the core are needed to enhance the stability of the mixed micelles. This requirement limits the choice of blending systems, which is not good for exploring new Janus architectures. However, Palyulin and Potemkin[23] demonstrated that homogeneous mixing of the soluble A and C blocks in the corona (mixed micelles) is also possible when the additional interactions between blocks in the core are absent. They found that the formation of pure or mixed micelles depends on the incompatibility between the A and C blocks.

In the current study, the self-assembly of an AB/BC diblock copolymer mixture in selective solvents for A and C blocks was examined *via* Monte Carlo (MC) simulation. In our simulations, no additional interaction between the insoluble B blocks was applied. The main purpose of this study is to reveal the effect of the control parameters, which includes the incompatibility between the solvophilic A and C blocks and the solvent quality for the solvophobic B block, on the formation of a Janus architecture.

Theoretical model

In this study, we used a lattice MC simulation to examine the formation of Janus micelles from the self-assembly of an AB/BC diblock copolymer mixture in a selective solution. MC simulation has proven to be an efficient method to study the solution-state self-assembly of copolymers, which include AB diblock copolymers,[24] ABA,[25,26] and ABC triblock copolymers,[27–30] ABC miktoarm star terpolymers,[31,32] and tetrablock copolymers.[33]

All simulations were carried out in a simple cubic lattice with a volume of $V = L \times L \times L$, where $L = 40$. This is because the computation time will be apparently increased as the box size further increases. In our previous study,[28] the effect of box size on the reproducibility of the micellar structure was examined. In that work, it was found that the representative micellar structures can be well reproduced in a $50 \times 50 \times 50$ simple cubic lattice. The periodic boundary condition was applied to all three directions. The single-site bond fluctuation model[34–36] was used; thus, the permitted bond length was either 1 or $\sqrt{2}$. Therefore, each site has 18 nearest neighbor sites. Excluded volume interactions were enforced to ensure that each lattice site in the lattice was occupied by either a polymer bead or a vacancy (solvent). In addition, bond crossing was forbidden. Evolution of the chain configuration was achieved through the exchange movements between the polymer bead and the solvent.

In the exchange move, a polymer bead is randomly selected to make an attempted exchange with one of its 18 nearest-neighbor sites. To improve the computation efficiency, the partial-reptation algorithm[37] is used in the simulation if the selected polymer bead was unable to make an exchange with any of the 18 nearest-neighbor sites because of a violation of the excluded volume conditions, the no-bond-crossing restrictions, or the bond length restrictions. If the attempted exchange move does not violate the aforementioned conditions and restrictions, the acceptance or rejection of the attempted move is further governed by the Metropolis rule,[38] wherein the exchange is accepted if the energy change ΔE is negative. Otherwise, the exchange is accepted with a probability of $p = \exp[-\Delta E/(k_B T)]$, where $\Delta E = \sum_{ij} \Delta N_{ij} \varepsilon_{ij}$; ΔN_{ij} is the number difference of the 18 nearest-neighbor pairs between components i and j before and after the exchange, where $i, j = A, B, C$ (polymer beads), or S (solvent). ε_{ij} is the reduced interaction between components i and j; k_B is the Boltzmann constant and is assumed to be 1, and T is the reduced temperature.

In this study, the self-assembly of an A_4B_6/B_6C_4 mixture was examined. The ratio of these two diblock copolymers was fixed at 1 : 1. Moreover, the volume fraction of the sum of A_4B_6 and B_6C_4 copolymers in the simulation box was fixed at 16%. The polymer–solvent interactions, ε_{AS} and ε_{CS}, were set to negative, whereas the solvent–polymer interaction, ε_{BS}, was set to positive to ensure that the solvents are poor to block B and good to blocks A and C. The polymer–polymer interactions ε_{AB}, ε_{AC}, and ε_{BC} were set to positive to mimic their incompatibilities. All the other self-interactions between the same components (*i.e.*, ε_{AA}, ε_{BB}, ε_{CC}, and ε_{SS}) were set to 0 for all the results.

The annealing method was implemented in the current study. This simulated annealing method is a well-known procedure for obtaining the low-energy stable states in complex systems, which is often used in computer simulations.[39,40] In the annealing process, $1/T$ gradually increases from 0 (an athermal state of $T = \infty$) to a given positive value at $1/T = 0.07$ (representing a state at a lower temperature), which was achieved in 350 steps at an annealing rate of 0.0002 per step. At each

annealing step, 9000 Monte Carlo steps (MCSs) were performed. One MCS means that on average, each bead has attempted one exchange move. After 350 annealing steps, $1/T$ was fixed at 0.07, and another sufficiently long period was taken. This annealing process corresponds to the experimental case that a selective solvent is slowly added in homogeneous AB/BC solution. To ensure that the final structures were in equilibrium state, all the simulations were performed with sufficiently long period running (over 1000 steps, each step includes 9000 Monte Carlo time). Moreover, all the micelles shown in the current study were obtained only when both the morphology and contact numbers between different components almost remain unchanged for a long time.

Results and discussion

In our simulation, the solvent quality was controlled by solvent–polymer interactions (*i.e.*, ε_{AS}, ε_{BS}, and ε_{CS}), whereas the incompatibility between the different block types was controlled by polymer–polymer interactions between different components (*i.e.*, ε_{AB}, ε_{AC}, and ε_{BC}). ε_{AS} and ε_{BS} were fixed at -1.0 to ensure that the A and C blocks are soluble in the solvents. The interactions between the solvophobic blocks (B blocks) and the solvophilic blocks (A or C blocks), *i.e.*, ε_{AB} and ε_{BC}, were fixed at 1.0. The effects of the incompatibility (ε_{AC}) between the solvophilic A and C blocks as well as the solvent quality for the solvophobic blocks (ε_{BS}) on the formation of Janus micelles were examined. Moreover, the pathway of some particular Janus micelles were also examined online.

1 Effect of ε_{AC} and ε_{BS} on the formation of Janus micelles

In Fig. 2, a series of resulting micellar morphologies are presented as a function of ε_{AC}, fixing ε_{BS} at 2.0. When $\varepsilon_{AC} = 3.0$, *i.e.*, the incompatibility between solvophilic A and C is relatively weak, spherical mixed micelles are formed in the mixture of A_4B_6/B_6C_4 copolymers (Fig. 2a), where the A and C blocks are homogeneously mixed within one corona. As the incompatibility between the A and C blocks increases ($\varepsilon_{AC} = 6.0$), microphase separation between the A and C blocks occurs, which leads to segregation of the corona into two distinct phases, *i.e.*, Janus spheres, as shown in Fig. 2b. However, a mixture of pure spherical micelles consisting of either AB or BC copolymers is observed as ε_{AC} further increases to 10.0 (Fig. 2c). This morphological transition from mixed to pure micelles is in agreement with the observation in Palyulin and Potemkin's study.[23] However, the intermediate architecture, *i.e.*, Janus architecture, is absent in that study. When the B blocks are moderately solvophobic in the selective solvents ($\varepsilon_{BS} = 6.0$), a different morphological transition from disk-like mixed micelles ($\varepsilon_{AC} = 0$) to cylindrical Janus micelles ($\varepsilon_{AC} = 3.0$) and finally to lamella-like Janus micelles ($\varepsilon_{AC} = 5.0$ and $\varepsilon_{AC} = 7.0$) can be observed in Fig. 3. When the solvophilic A and C blocks are completely compatible (*i.e.*, $\varepsilon_{AC} = 0$), a flat disk with a mixed corona is formed in the A_4B_6/B_6C_4 mixture (Fig. 3a). By slightly increasing ε_{AC} to 3.0, the A_4B_6/B_6C_4 mixture is more likely to aggregate into a cylindrical Janus micelle with two discernible faces (Fig. 3b). A morphological transition from a Janus cylinder to a Janus lamella is observed when ε_{AC} is further increased to 5.0 (Fig. 3c). This lamella-like

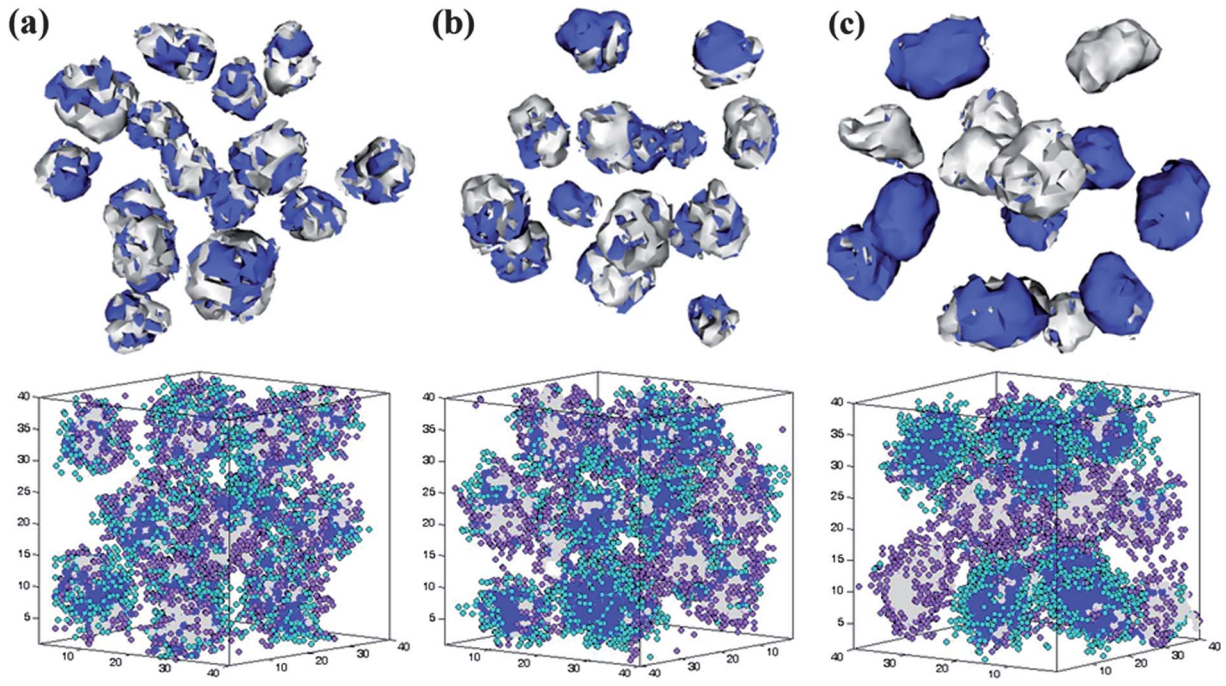

Fig. 2 Morphologies of the A_4B_6/B_6C_4 mixture in a selective solvent as a function of ε_{AC}. ε_{BS} is fixed at 2.0. (a) $\varepsilon_{AC} = 3.0$; (b) $\varepsilon_{AC} = 6.0$; (c) $\varepsilon_{AC} = 10.0$. The top images are the morphologies of the density distributions of the solvophobic B blocks in the resulting micelles. The bottom images are the snapshots of the resulting micelles. □ and ■ represent the solvophobic B blocks from AB and BC block copolymers, respectively; ■ and ■ represent the solvophilic A and C blocks from AB and BC block copolymers, respectively.

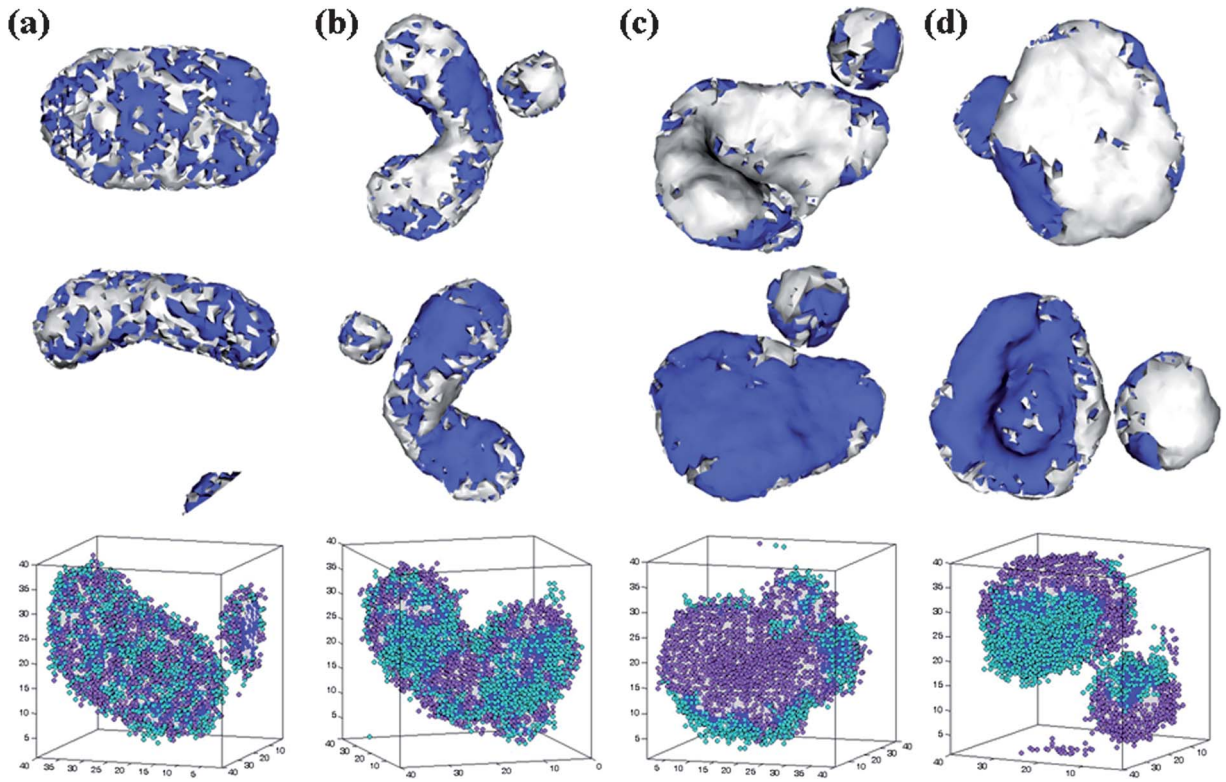

Fig. 3 Morphologies of the A_4B_6/B_6C_4 mixture in a selective solvent as a function of ε_{AC}. ε_{BS} is fixed at 6.0. (a) $\varepsilon_{AC} = 0$; (b) $\varepsilon_{AC} = 3.0$; (c) $\varepsilon_{AC} = 5.0$; (d) $\varepsilon_{AC} = 7.0$. The top images are the morphologies of the density distributions of the solvophobic B blocks in the resulting micelles. The bottom images are the snapshots of the resulting micelles. The color codes of the morphologies are the same as that in Fig. 2.

Janus structure remains mostly unchanged as ε_{AC} further increases to 7.0 (Fig. 3d). A similar cylinder-like Janus structure and the lamella-like Janus structure were also obtained by Müller and co-workers.[15,17] However, these two interesting Janus structures were generated from selective cross-linking of the central block, and then redissolution of the lamellae-cylinder and lamellae–lamellar structure obtained from the bulk self-assembly of block terpolymers in their study. No previous study has reported on the formation of Janus cylinder and Janus lamella from the solution self-assembly of block copolymers.

When $\varepsilon_{BS} = 10.0$, that is, the B blocks are highly insoluble in the selective solvents, vesicles are obtained, as shown in Fig. 4a–d. Fig. 4a shows that when $\varepsilon_{AC} = 0$, the A_4B_6/B_6C_4 mixture aggregates into a spherical mixed vesicle. From the cross-section image in Fig. 4a, the soluble A and C blocks are randomly distributed on the surfaces of the vesicle. As ε_{AC} slightly increases to 3.0 (Fig. 4b), the vesicle shape changes from spherical to ellipsoidal because the A and C coronas tend to move away from each other to decrease their contact, which causes the micellar shape change from sphere to ellipsoid. The cross-section image in Fig. 4b shows that only one kind of solvophilic block (it is the A-type block in Fig. 4b, which depends on the initial state) is located on the inner surface of the vesicle. When ε_{AC} further increases to 5.0, the microphase separation between the soluble A and C blocks becomes increasingly evident. As a result, a Janus vesicle with a two-faced corona is formed in the A_4B_6/B_6C_4 mixture (Fig. 4c). The Janus-like vesicle structure remains unchanged as ε_{AC} increases from 5.0 to 7.0 as shown in Fig. 4d. Jiang and coworkers observed a similar transition from a symmetric vesicle to a Janus vesicle by increasing the incompatibility between A and C blocks in the self-assembly of an AB/BC diblock copolymer mixture based on hydrogen bonding between the two ends of the two B blocks.[18] However, the Janus vesicle in the present study is generated from an AB/BC diblock copolymer mixture with no additional interaction between the insoluble B blocks.

In the simulations, the solvent quality was controlled by the interactions between the solvophobic B blocks and the solvents (*i.e.*, ε_{BS}). A series of aggregated morphologies of the A_4B_6/B_6C_4 mixture at different ε_{BS} with fixed ε_{AC} values at 5.0 (Fig. 5) and 10.0 (Fig. 6), respectively, are presented to examine the effect of the solvent quality on the formation of Janus micelles from the A_4B_6/B_6C_4 mixture. When the incompatibility between the different solvophilic block types is relatively moderate ($\varepsilon_{AC} = 5.0$, Fig. 5), a morphological sequence, *i.e.*, Janus sphere ($\varepsilon_{BS} = 5.0$) → Janus lamella ($\varepsilon_{BS} = 6.0$) → Janus ring ($\varepsilon_{BS} = 6.196$) → Janus cylinder ($\varepsilon_{BS} = 6.2$) → Janus vesicle ($\varepsilon_{BS} = 10.0$), is observed when the solvent quality for the solvophobic segments decreases. In this morphological transition, a novel Janus micellar structure, that is, a Janus ring (Fig. 5c), is predicted for the first time, which corresponds to the Janus structure illustrated in Fig. 1h. Moreover, we also

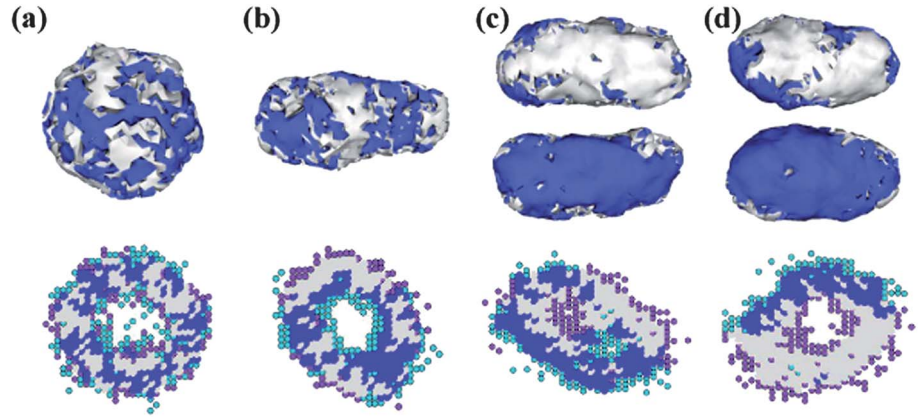

Fig. 4 Morphologies of the A_4B_6/B_6C_4 mixture in a selective solvent as a function of ε_{AC}. ε_{BS} is fixed at 10.0. (a) $\varepsilon_{AC} = 0$; (b) $\varepsilon_{AC} = 3.0$; (c) $\varepsilon_{AC} = 5.0$; (d) $\varepsilon_{AC} = 7.0$. The top images are the morphologies of the density distributions of the solvophobic B blocks in the resulting micelles. The bottom images are the cross-section snapshots of the resulting micelles. The color codes of the morphologies are the same as that in Fig. 2.

observed another interesting Janus micellar structure, *i.e.*, a Janus cylinder (Fig. 5d, as illustrated in Fig. 1d), which is in agreement with existing experimental observations.[14,15] However, in the existing experimental studies, the Janus cylinder was obtained from the lamellae-cylinder morphology from the bulk self-assembly of the polystyrene-*b*-polybutadiene-*b*-poly(methyl methacrylate) (PS-PB-PMMA) terpolymer. A different morphological sequence, namely, Janus disk ($\varepsilon_{BS} = 6.0$) → Janus cylinder ($\varepsilon_{BS} = 6.196$) → Janus spheres ($\varepsilon_{BS} = 7.0$) → Janus lamella ($\varepsilon_{BS} = 8.0$) → Janus vesicles ($\varepsilon_{BS} = 10.0$), is observed for $\varepsilon_{AC} = 10.0$ when the solvent quality for the solvophobic segments decreases, as shown in Fig. 6. In this morphological transition, a novel lamella-like Janus micelle is observed when $\varepsilon_{BS} = 8.0$ (Fig. 6d). Both sides of the lamella show a Janus pattern. Similarly, the front and the back of the lamella also display a Janus structure. To the best of our knowledge, this complex Janus lamella structure has not been observed yet.

A phase diagram of ε_{AC} and ε_{BS} is shown in Fig. 7 to understand the effects of ε_{AC} and ε_{BS} on the formation of Janus architecture. In the current study, the micellar morphology of each state point in the phase diagram was obtained from a single simulation. This is because the resulting micellar structures are independent of the initial states, when their initial states are homogenous. For example, the A_4B_6/B_6C_4 mixtures can aggregate into Janus cylinder ($\varepsilon_{AC} = 5.0$ and $\varepsilon_{BS} = 6.2$, Fig. 5d), Janus lamella ($\varepsilon_{AC} = 7.0$ and $\varepsilon_{BS} = 6.0$, Fig. 3d) and Janus vesicle ($\varepsilon_{AC} = 7.0$ and $\varepsilon_{BS} = 10.0$, Fig. 4d), respectively.

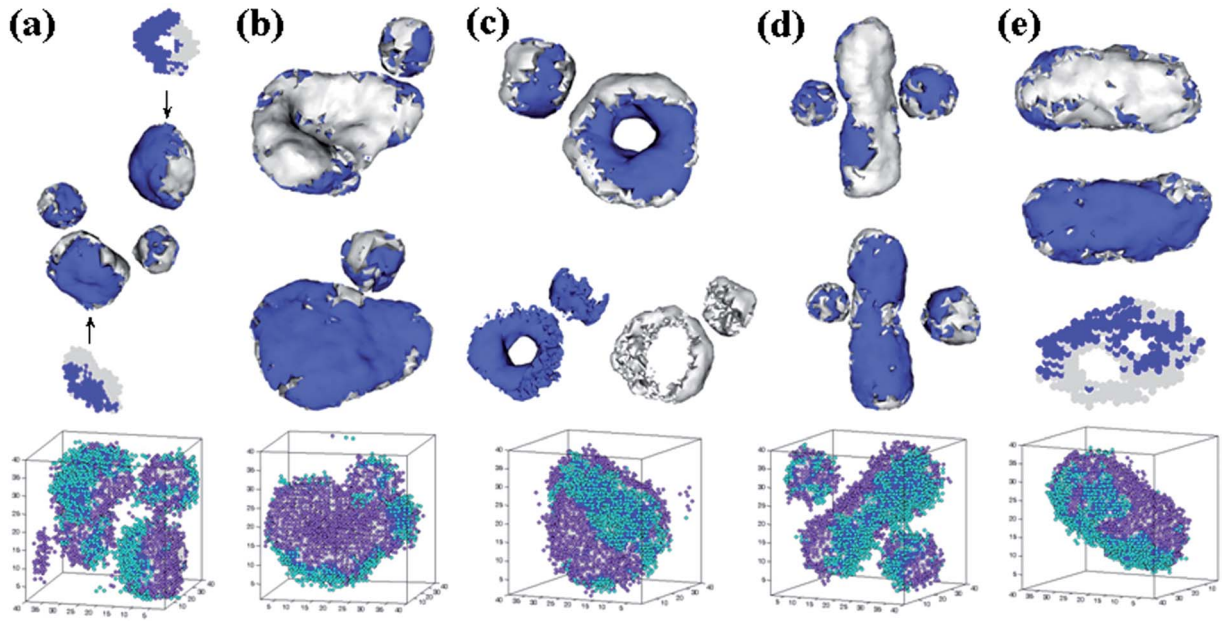

Fig. 5 Morphologies of the A_4B_6/B_6C_4 mixture in a selective solvent as a function of ε_{BS}. ε_{AC} is fixed at 5.0. (a) $\varepsilon_{BS} = 5.0$; (b) $\varepsilon_{BS} = 6.0$; (c) $\varepsilon_{BS} = 6.196$; (d) $\varepsilon_{BS} = 6.2$; (e) $\varepsilon_{BS} = 10.0$. The top images are the morphologies of the density distributions of the solvophobic B blocks in the resulting micelles. The bottom images are the snapshots of the resulting micelles. The color codes of the morphologies are the same as that in Fig. 2.

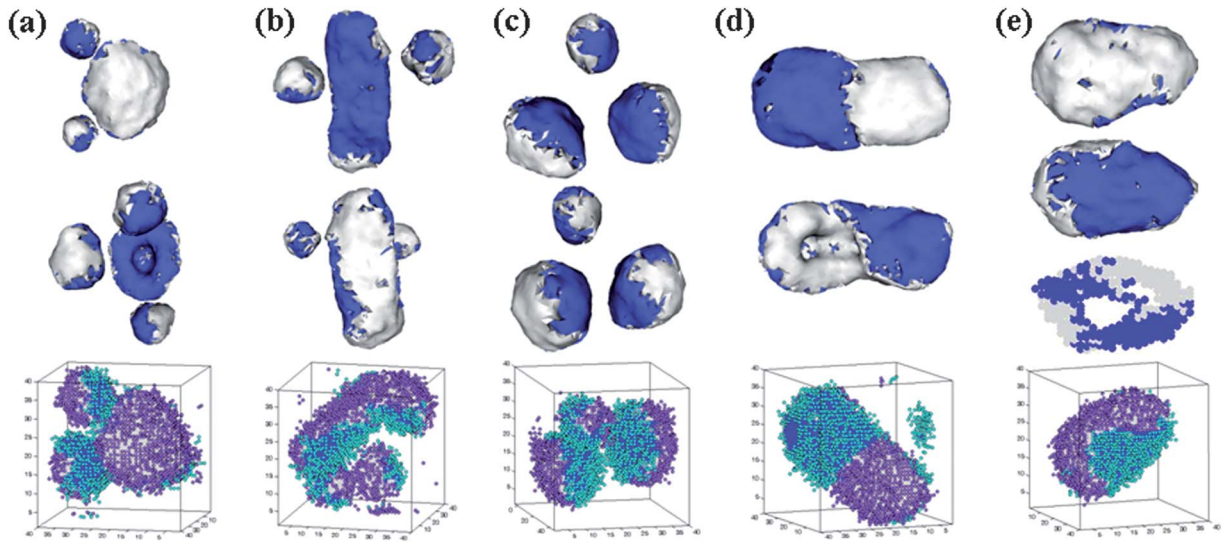

Fig. 6 Morphologies of the A_4B_6/B_6C_4 mixture in a selective solvent as a function of ε_{BS}. ε_{AC} is fixed at 10.0. (a) $\varepsilon_{BS} = 6.0$; (b) $\varepsilon_{BS} = 6.196$; (c) $\varepsilon_{BS} = 7.0$; (d) $\varepsilon_{BS} = 8.0$; (e) $\varepsilon_{BS} = 10.0$. The top images are the morphologies of the density distributions of the solvophobic B blocks in the resulting micelles. The bottom images are the snapshots of the resulting micelles. The color codes of the morphologies are the same as that in Fig. 2.

Using a different homogeneous state as the initial state, these three representative micellar structures were well reproduced (Fig. S1, ESI†). Despite the variety of micellar morphologies shown in the phase diagram, several common features can be extracted from it. First, the mixed micelles are located on the left of the phase diagram, whereas the Janus micelles are

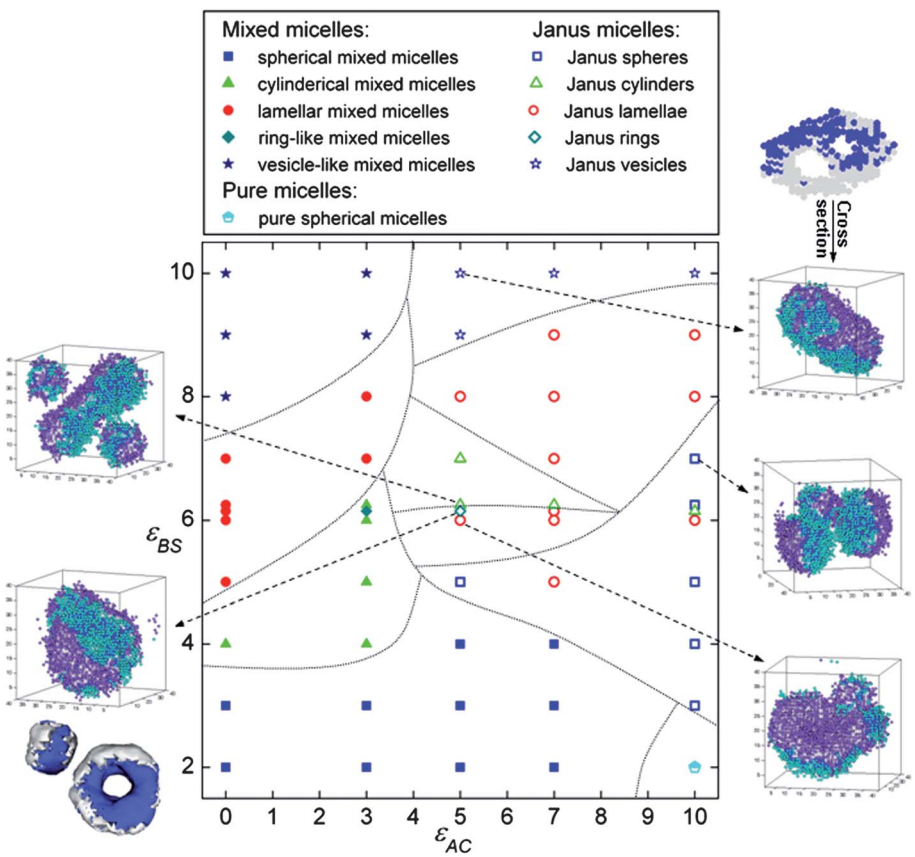

Fig. 7 Morphological phase diagram of the A_4B_6/B_6C_4 mixture in a selective solvent. Several representative snapshots of the Janus micelles are inserted in the diagram. The color codes of the inserted snapshots are the same as that in Fig. 2.

located on the right portion of the phase diagram. This result implies that ε_{AC} has a key function in the formation of Janus architecture from the self-assembly of the AB/BC mixture in the A and C selective solvents. In addition, the mixed micelles are found on the lower-middle of the phase diagram, which indicates that it is difficult to form a Janus architecture when the B block is weakly insoluble in the selective solvents. Second, as the solvent quality for the B blocks decreases (*i.e.*, ε_{BS} increases), a morphological transition from sphere to cylinder to lamella and then to vesicle is observed either in the mixed-micelle region or in the Janus-micelle region. These resulting micelles can be divided into zero-dimensional (spherical micelles), one-dimensional (cylindrical micelles), two-dimensional (lamellar micelles), and three-dimensional (vesicles) structures. The morphological sequence of sphere → cylinder → lamella → vesicle is in agreement with our previous work,[28] *i.e.*, the micellar structures transform from low- to high-dimensional micelles when the solvent quality for the solvophobic B blocks decreases. This result indicates that the micellar shape or dimension is controlled only by the solvent quality.

2 Formation pathways of Janus-like ring, lamella, and vesicle

Until now, the dynamic formation process of Janus micelles remains unclear because of the limitations in experimental technique. In this section, the formation pathways and the growth mechanisms of particular Janus micelles such as Janus-like ring, lamella, and vesicle are examined. Fig. 8 presents the variations of numbers of contacts (N_{BS} and N_{AC}) with MC time for the A_4B_6/B_6C_4 mixture at $\varepsilon_{BS} = 6.196$ and $\varepsilon_{AC} = 5.0$. N_{BS} is the contact number between the B-type monomers and the solvents, which indicates the micellization degree of the solvophobic B blocks in the selective solvents. N_{AC} represents the contact number between the A- and C-type monomers, and corresponds to the microphase-separation degree between the solvophobic A and C blocks. Several typical snapshots at different times are also inserted in Fig. 8 to show the formation pathway of the ring-shaped Janus micelles. The snapshots (a)–(d) show that the A_4B_6/B_6C_4 mixture aggregates into mixed cylindrical micelles at first (snapshot (b), $t = 90$) and then transforms into a ring-shaped micelle (snapshot (c), $t = 130$). The micellar shape then remains unchanged but the inner structure changes into a Janus structure (snapshot (d), $t = 350$). The variations in N_{BS} and N_{AC} with time are consistent with the formation pathway of the Janus ring-shaped micelle. From the N_{BS}–t curve, N_{BS} shows a steady decline with time until micellization is completed (snapshot (c), $t = 130$), and then remains mostly unchanged during the transition from the mixed ring-shaped micelle to the Janus ring-shaped micelle. For the N_{AC}–t curve, N_{AC} remarkably increases with time during micellization of the mixed ring-shaped micelle (snapshot (c), $t = 130$), and then significantly declines when the mixed ring-shaped micelle changes to the Janus ring-shaped micelle (snapshot (d), $t = 350$). After formation of the Janus ring-shaped micelle, N_{AC} remains mostly unchanged until the end of the simulation (snapshot (e), $t = 1044$).

Fig. 9 shows the formation pathway of the Janus vesicle from the self-assembly of the A_4B_6/B_6C_4 mixture. As shown in the snapshots at different times, the A_4B_6/B_6C_4 mixture first forms a mixed ring-shaped micelle (snapshot (b), $t = 75$), and then shrinks to a Janus lamellar micelle (snapshot (c), $t = 100$). As time is further increased, the Janus lamella transforms into a Janus vesicle because some hydrophilic molecules diffuse toward the center (snapshot (d), $t = 140$).[25] Subsequently, the hydrophilic molecules continue to diffuse

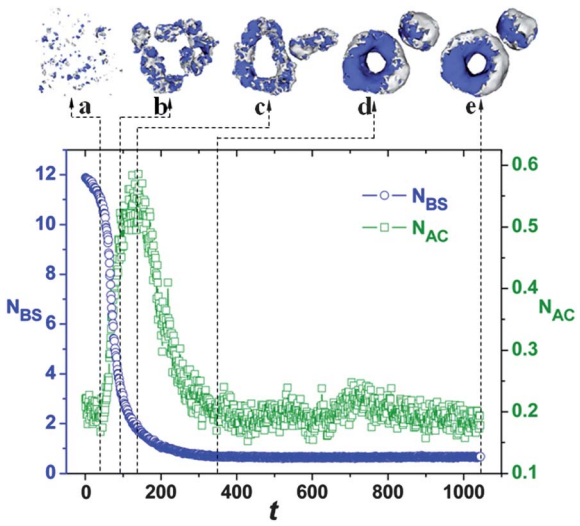

Fig. 8 Variations in the contact numbers, N_{BS} and N_{AC}, with time during the formation of ring-shaped Janus micelles. ε_{BS} and ε_{AC} are fixed at 6.196 and 5.0, respectively. Several typical snapshots at different times are inserted in the curves to show the formation pathway of the ring-shaped Janus micelles. The color codes of the inserted snapshots are the same as that in Fig. 2. (a) $t = 40$; (b) $t = 90$; (c) $t = 130$; (d) $t = 350$; (e) $t = 1044$.

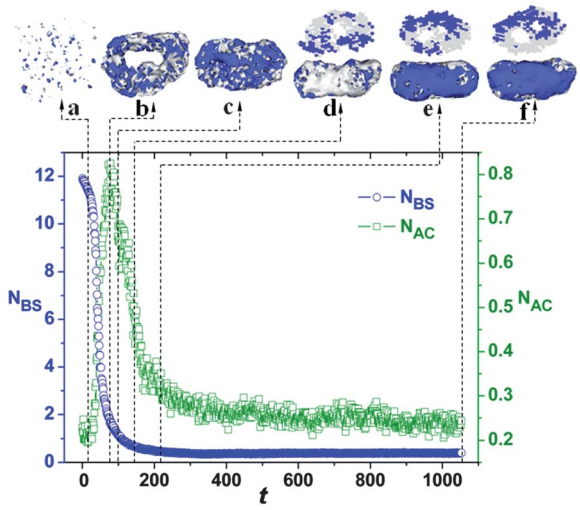

Fig. 9 Variations in the contact numbers, N_{BS} and N_{AC}, with time during the formation of the vesicle-shaped Janus micelles. ε_{BS} and ε_{AC} are fixed at 10.0 and 5.0, respectively. Several typical snapshots at different times are inserted in the curves to show the formation pathway of the vesicle-shaped Janus micelles. The color codes of the inserted snapshots are the same as that in Fig. 2. (a) $t = 20$; (b) $t = 75$; (c) $t = 100$; (d) $t = 140$; (e) $t = 220$; (f) $t = 1053$.

toward the center of the micelles, which leads to the appearance of another compartment inside the Janus vesicle (snapshot (e), $t = 220$). The variations in contact numbers, N_{BS} and N_{AC}, with time are also given in Fig. 9. No significant difference can be observed between the curves of N_{BS}–t and N_{AC}–t in Fig. 8 and 9. Similarly, N_{BS} significantly decreases with time during micellization of the A_4B_6/B_6C_4 mixture (snapshots (a) and (b)) and then remains almost unchanged during the micellar transitions (snapshots (b)–(f)), whereas N_{AC} increases to a maximum value (snapshots (a) and (b)) and then declines (snapshots (b)–(f)). The kinetic process of Janus lamella from the A_4B_6/B_6C_4 mixture is shown in Fig. 10 through a series of snapshots of the micelles at different times. The variations in contact numbers, N_{BS} and N_{AC}, with time are also given in Fig. 10 to illustrate the formation mechanism of the lamella-like Janus micelle quantitatively. From the snapshots (a)–(e), the formation pathway of the Janus lamella is from a mixed cylinder to a mixed lamella and then to a Janus lamella. The N_{BS}–t and N_{AC}–t curves shown in Fig. 10 are consistent with the formation pathway of the lamella-like Janus micelle. The A_4B_6/B_6C_4 mixture aggregates into a mixed cylindrical micelle and N_{AC} reaches its peak value at $t = 125$ (snapshot (b)). Thereafter, N_{AC} starts to decrease when the mixed cylinder (snapshot (b), $t = 125$) changes to a bent Janus cylinder (snapshot (c), $t = 400$) and then into a Janus lamella (snapshot (d), $t = 700$). For the N_{BS}–t curve, N_{BS} first decreases with time during aggregation of the A_4B_6/B_6C_4 mixture into a mixed cylindrical micelle, and then remains almost unchanged when the mixed cylindrical micelle transitions into a bent Janus cylinder and finally to a Janus lamellar micelle. From the formation pathways of various Janus micelles shown in Fig. 8–10, the micellization of solvophobic B blocks occurs before the microphase separation between the solvophobic A and C blocks.

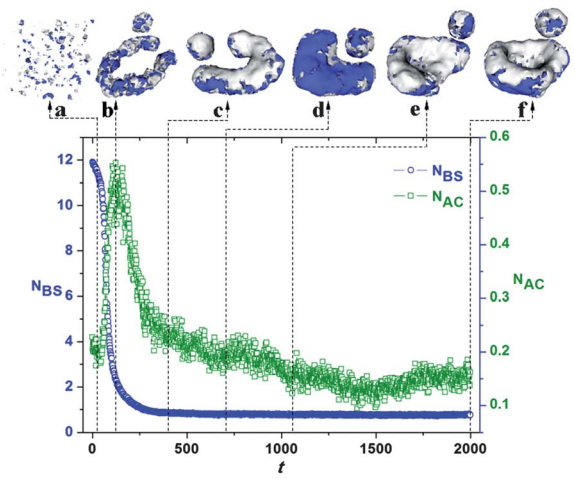

Fig. 10 Variations in the contact numbers, N_{BS} and N_{AC}, with time during the formation of disk-shaped Janus micelles. ε_{BS} and ε_{AC} are fixed at 6.0 and 5.0, respectively. Several typical snapshots at different times are inserted in the curves to show the formation pathway of the disk-shaped Janus micelles. The color codes of the inserted snapshots are the same as that in Fig. 2. (a) $t = 40$; (b) $t = 125$; (c) $t = 400$; (d) $t = 700$; (e) $t = 1060$; (f) $t = 1999$.

Conclusion

We investigated the self-assembly of amphiphilic A_4B_6/B_6C_4 copolymers in A and C block-selective solvents using the MC technique. Although no additional attractive interactions between the insoluble B blocks were applied, various Janus-like micelles, such as Janus sphere, cylinder, lamella, vesicle, and ring, are observed. To understand the formation of Janus micelles comprehensively, the influence of two important control parameters, namely, the solvent quality for the solvophobic B blocks (ε_{BS}) and the incompatibility between the solvophilic A and C blocks (ε_{AC}), on the micellar structure were systematically investigated, and a generic phase diagram in $\varepsilon_{BS} \times \varepsilon_{AC}$ was constructed and discussed. From the phase diagram, several generic features can be identified. The micellar shape is mainly controlled by ε_{BS}, whereas the formation of the Janus architecture is largely controlled by ε_{AC}. As the solvent quality for the solvophobic B blocks decreases, the micellar structures transform from low- to high-dimensional micelles. In addition, the formation pathways of particular Janus micellar structures, such as Janus ring, vesicle, and lamella, are elucidated and illustrated. It was also found that the micellization of solvophobic B blocks occurs before the microphase separation between the solvophobic A and C blocks during the formation of Janus micelles.

Acknowledgements

This work was financially supported by the National Natural Science Foundation of China for Youth Science Funds (21104083), the Scientific Development Program of Jilin Province (201201007) and the Open Project of State Key Laboratory of Supramolecular Structure and Materials (sklssm201331).

References

1 P. A. Suci, S. Kang, M. Young and T. Douglas, *J. Am. Chem. Soc.*, 2009, **131**, 9164–9165.
2 H. Xie, Z.-G. She, S. Wang, G. Sharma and J. W. Smith, *Langmuir*, 2012, **28**, 4459–4463.
3 H. Xing, Z. D. Wang, Z. D. Xu, N. Y. Wong, Y. Xiang, G. L. G. Liu and Y. Lu, *ACS Nano*, 2012, **6**, 802–809.
4 D. J. Cole-Hamilton, *Science*, 2010, **327**, 41–42.
5 Z. F. Li, D. Y. Lee, M. F. Rubner and R. E. Cohen, *Macromolecules*, 2005, **38**, 7876–7879.
6 L. Y. Wu, B. M. Ross, S. Hong and L. P. Lee, *Small*, 2010, **6**, 503–507.
7 C. J. Behrend, J. N. Anker, B. H. McNaughton, M. Brasuel, M. A. Philbert and R. Kopelman, *J. Phys. Chem. B*, 2004, **108**, 10408–10414.
8 P. G. de Gennes, *Rev. Mod. Phys.*, 1992, **64**, 645–648.
9 R. Erhardt, M. Zhang, A. Böker, H. Zettl, C. Abetz, P. Frederik, G. Krausch, V. Abetz and A. H. E. Müller, *J. Am. Chem. Soc.*, 2003, **125**, 3260–3267.
10 R. Erhardt, A. Böker, H. Zettl, H. Kaya, W. Pyckhout-Hintzen, G. Krausch, V. Abetz and A. H. E. Müller, *Macromolecules*, 2001, **34**, 1069–1075.

11 A. Walther, C. Barner-Kowollik and A. H. E. Müller, *Langmuir*, 2010, **26**, 12237–12246.
12 J. W. Hu and G. J. Liu, *Macromolecules*, 2005, **38**, 8058–8065.
13 Y. Han and W. Jiang, *J. Phys. Chem. B*, 2011, **115**, 2167–2172.
14 A. Walther, M. Drechsler, S. Rosenfeldt, L. Harnau, M. Ballauff, V. Abetz and A. H. E. Müller, *J. Am. Chem. Soc.*, 2009, **131**, 4720–4728.
15 Y. Liu, V. Abetz and A. H. E. Müller, *Macromolecules*, 2003, **36**, 7894–7898.
16 I. K. Voets, A. de Keizer, P. de Waard, P. M. Frederik, P. H. H. Bomans, H. Schmalz, A. Walther, S. M. King, F. A. M. Leermakers and M. A. Cohen Stuart, *Angew. Chem., Int. Ed.*, 2006, **45**, 6673–6676.
17 A. Walther, X. André, M. Drechsler, V. Abetz and A. H. E. Müller, *J. Am. Chem. Soc.*, 2007, **129**, 6187–6198.
18 Y. Han, J. Cui and W. Jiang, *J. Phys. Chem. B*, 2012, **116**, 9208–9214.
19 A. M. Jackson, J. W. Myerson and F. Stellacci, *Nat. Mater.*, 2004, **3**, 330–336.
20 B. Wang, B. Li, B. Zhao and C. Y. Li, *J. Am. Chem. Soc.*, 2008, **130**, 11594–11595.
21 I. C. Pons-Siepermann and S. C. Glotzer, *Soft Matter*, 2012, **8**, 6226–6231.
22 J. Du and S. P. Armes, *Soft Matter*, 2010, **6**, 4851–4857.
23 V. V. Palyulin and I. I. Potemkin, *Macromolecules*, 2008, **41**, 4459–4463.
24 P. Sun, Y. Yin, B. Li, T. Chen, Q. Jin, D. Ding and A.-C. Shi, *J. Chem. Phys.*, 2005, **122**, 204905.
25 Y. Han, H. Yu, H. Du and W. Jiang, *J. Am. Chem. Soc.*, 2010, **132**, 1144–1150.
26 W. Kong, B. Li, Q. Jin, D. Ding and A.-C. Shi, *Langmuir*, 2010, **26**, 4226–4232.
27 J. Cui and W. Jiang, *Langmuir*, 2010, **26**, 13672–13676.
28 Y. Zhu, H. Yu, Y. Wang, J. Cui, W. Kong and W. Jiang, *Soft Matter*, 2012, **8**, 4695–4707.
29 Y. Zhu, X. Yang, W. Kong, Y. Sheng and N. Yan, *Soft Matter*, 2012, **8**, 11156–11162.
30 W. Kong, W. Jiang, Y. Zhu and B. Li, *Langmuir*, 2012, **28**, 11714–11724.
31 Y. Zhu, R. K. Y. Li and W. Jiang, *Chem. Phys.*, 2006, **327**, 137–143.
32 W. Kong, B. Li, Q. Jin, D. Ding and A.-C. Shi, *J. Am. Chem. Soc.*, 2009, **131**, 8503–8512.
33 J. Cui and W. Jiang, *Langmuir*, 2011, **27**, 10141–10147.
34 I. Carmesin and K. Kremer, *Macromolecules*, 1988, **21**, 2819–2823.
35 R. G. Larson, *J. Chem. Phys.*, 1988, **89**, 1642–1650.
36 R. G. Larson, *J. Chem. Phys.*, 1992, **96**, 7904–7918.
37 S. Ji and J. Ding, *Langmuir*, 2006, **22**, 553–559.
38 N. Metropolis, A. W. Rosenbluth, M. N. Rosenbluth, A. H. Teller and E. Teller, *J. Chem. Phys.*, 1953, **21**, 1087–1092.
39 S. Kirkpatrick, C. D. Gelatt and M. P. Vecchi, *Science*, 1983, **220**, 671–680.
40 G. S. Grest, C. M. Soukoulis and K. Levin, *Phys. Rev. Lett.*, 1986, **56**, 1148–1151.

